

LETTER TO THE EDITOR

Discriminating Planck Reionisation Histories with the kSZ Effect

M. Douspis^{1,2} *, A. Gorce¹, S. Ilić³, L. McBride⁴, M. Muñoz-Echeverría⁶, E. Pointecouteau⁷, L. Salvati¹, and M. Tristram⁵

¹ Université Paris-Saclay, CNRS, Institut d'Astrophysique Spatiale, 91405 Orsay, France

² Observatoire de Paris, PSL Research University, Sorbonne Université, CNRS, LUX, 75014 Paris, France

³ Institut du Développement et des Ressources en Informatique Scientifique (IDRIS), CNRS, Université Paris-Saclay, Orsay, France

⁴ Université Paris-Saclay, Inria, Inria Saclay-Île-de-France, 91120, Palaiseau, France.

⁵ IJCLab, Université Paris-Saclay, CNRS/IN2P3, IJCLab, 91405 Orsay, France

⁶ Institut de Radioastronomie Millimétrique (IRAM), Avenida Divina Pastora 7, Local 20, E-18012, Granada, Spain

⁷ IRAP, CNRS, Université de Toulouse, CNES, UT3-UPS, Toulouse, France

Received December 25, 20XX

ABSTRACT

The epoch of reionisation is a key phase in cosmic history, but its detailed evolution remains poorly constrained by current cosmic microwave background (CMB) observations. We investigate whether the kinetic Sunyaev–Zel’dovich (kSZ) effect can discriminate among reionisation histories consistent with current large-scale CMB constraints. Using histories derived from Planck data, we compute the corresponding kSZ angular power spectra within an analytical framework, separating late-time and patchy contributions and accounting for uncertainties in both the ionisation history, $x_e(z)$, and astrophysical parameters constrained by the LORELI II simulations. The allowed histories fall into two broad classes, ‘short’ and ‘long’ duration reionisation, yielding distinct kSZ signatures. Uncertainties from $x_e(z)$ and astrophysical parameters produce comparable amount of dispersion, yet the two classes remain clearly separable, with variations within each class at the $\sim 10\%$ level. Current kSZ measurements ($\sim 0\text{--}3 \mu\text{K}^2$) are not yet precise enough to distinguish between these scenarios, although they tend to favor a ‘short’ reionisation. The kSZ effect thus provides a promising probe of reionisation beyond optical depth constraints. In particular, a measurement of the kSZ power spectrum at $\ell \sim 2000$ with $\sim 0.4 \mu\text{K}^2$ sensitivity would discriminate between ‘short’ and ‘long’ reionisation scenarios.

Key words. Reionisation – CMB – kinetic SZ

1. Introduction

The epoch of reionisation marks a pivotal phase in cosmic history, during which the first galaxies emitted sufficient ultraviolet radiation to ionise the intergalactic medium (IGM), ending the cosmic Dark Ages. Understanding the timing, duration, and sources of reionisation remains a key challenge in modern cosmology. Observations of the cosmic microwave background (CMB) by the *Planck* satellite, in temperature and polarisation, have provided crucial constraints on the optical depth to reionisation (Planck Collaboration Int. XLVII 2016; Ilić et al. 2025), offering an overall view of this process. However, these measurements are limited by the integrated nature of the signal allowing us to constrain a range of possible reionisation histories.

Recent observations with high-resolution CMB experiments have opened a new window on reionisation through the measurement of the kinematic Sunyaev–Zel’dovich effect (kSZ, Zeldovich & Sunyaev 1969; Sunyaev & Zeldovich 1980) at small angular scales. The kSZ effect, arising from the scattering of CMB photons by free electrons in moving ionised gas, is sensitive to the distribution and velocity of ionised matter during and after reionisation. By probing the kSZ signal at arcminute scales, upcoming and current CMB experiments can in theory constrain the duration, patchiness and inhomogeneity of reionisation, complementing *Planck*’s large-scale data

(e.g. Zahn et al. 2012; Planck Collaboration Int. XLVII 2016; Reichardt et al. 2021; Beringue et al. 2025; Chaubal et al. 2026).

In this work, we investigate whether the kSZ signatures of the reionisation histories allowed by the latest *Planck* data (Ilić et al. 2025), are distinct enough for current experiments to already differentiate between them. We assume a fixed cosmology through this article corresponding to ‘‘Planck (baseline)’’ column in (Tristram et al. 2026, Table 1).

2. The kSZ angular power spectrum

The kinetic Sunyaev–Zel’dovich effect is composed of two distinct contributions: a late-time component, arising from bulk flows of ionised gas after the completion of reionisation, and a patchy component, generated during reionisation itself as ionised bubbles form and expand in the IGM. The latter encodes most of the information about the timing, duration, and morphology of cosmic reionisation.

2.1. Modelling patchy kSZ

To model the patchy kSZ angular power spectrum (APS) we follow the analytical approach of Gorce et al. (2020), which relies on two main ingredients: the reionisation history, $x_e(z)$, and the electron overdensity power spectrum, which shape is parametrised with an amplitude at large scale α_0 and a cutoff scale κ (loosely related to a typical ionised bubble size)

* marian.douspis@universite-paris-saclay.fr

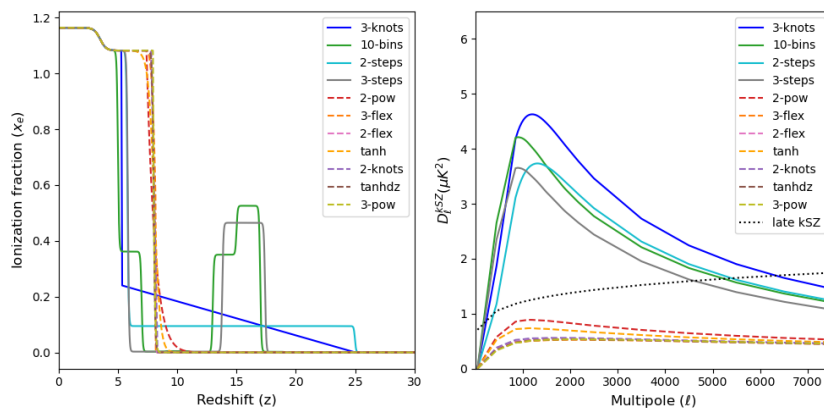


Fig. 1: Reionisation history (left) and corresponding patchy- (solid and dashed) and late- (dotted) kSZ angular power spectra. Solid (dashed) lines show the ‘long’ (‘short’) reionisation histories. Labels are defined in the text.

2.1.1. Histories of reionisation from *Planck*

Ilić et al. (2025) tested different parameterisations of the reionisation history with 1 to 12 free parameters. They used the latest *Planck* PR4 CMB data (Planck Collaboration Int. LVII 2020) to constrain the reionisation history of the Universe, systematically evaluating a wide range of models, from simple parametric to flexible non-parametric approaches. Their analysis, employing both Bayesian and frequentist methods, yields robust and consistent estimates of the reionisation optical depth. Using a frequentist approach, the authors obtain $\tau = 0.0581 \pm 0.0061 \pm 0.0005$, where the first uncertainty represents the statistical error and the second corresponds to the systematic error associated with x_e modelling. This systematic uncertainty, together with that arising from the assumed foreground models (Tristram et al. 2026), is negligible in comparison with the current statistical uncertainty. These results suggest that reionisation was a relatively recent process (see Fig. 1); a conclusion reached in other studies based on CMB data (e.g. Planck Collaboration Int. XLVII 2016; Planck Collaboration VI 2020; Pagano et al. 2020; Paradiso et al. 2023; Planck Collaboration Int. LVII 2020; Genesini et al. 2026). We choose to consider the best fit $x_e(z)^{\text{best}}$ for each model obtained with the frequentist approach in Ilić et al. (2025) as our inputs when deriving the kSZ APS¹.

Parameterisations are labelled following Ilić et al. (2025): hyperbolic tangent models with 1 or 2 free parameters (tanh, tanhdz); power-law models with 2 or 3 free parameters (pow-2, pow-3); step-based models with 2 or 3 steps (2-steps and 3-steps); interpolation-based models with 2 or 3 nodes (2-knots, 3-knots for the linear interpolation, and 2-flex, 3-flex for the PCHIP interpolation); binned models (10-bins). The corresponding reionisation histories are plotted in Fig. 1 (left) and can be split into two groups, depending on the ‘duration’ of the reionisation epoch ($\Delta z \equiv z(x_{e,90}) - z(x_{e,10})$)². Models with ‘long’ reionisation phases ($\Delta z > 2$) are plotted in solid lines while ‘short’ reionisation models ($\Delta z < 2$) are plotted in dashed lines.

Modelling uncertainties. To propagate the uncertainty on the history of reionisation to the kSZ APS, we use, for each param-

¹ We exclude the PCA parameterisation from Ilić et al. (2025), as it contains negative values and are left with 11 models.

² $x_{e,90}$ ($x_{e,10}$) is defined as the last (first) time the reionisation history reaches 90% (10%) respectively.

eterisation, all $x_e(z)$ models that satisfy $\chi^2 < \chi^2(x_e(z)^{\text{best}}) + 1$ (intervals plotted in dashed red lines in Fig. 6 of Ilić et al. 2025). The ensemble envelop of all the derived kSZ APS is defined as our 68% interval around our fiducial kSZ spectra.

2.1.2. Electron overdensity for LORELI II

The parameters α_0 and κ are *a priori* unknown, and we choose to consider the range of possibilities provided by the LORELI II suite of simulations (Meriot & Semelin 2024; Meriot et al. 2025). The $\sim 10,000$ simulations are generated by varying five astrophysical parameters that impact the ionising properties of galaxies. Two parameters that describe their X-ray production have been shown to have little impact on the kSZ spectrum amplitude and shape (see Appendix C in McBride et al. 2025) and are thus fixed. The three remaining parameters describe the source properties: the Gas Conversion Timescale governs how efficiently galaxies turn gas into stars; the Minimum Halo Mass defines the critical mass above which the star formation is sufficient to produce enough ionising radiation to form bubbles; the Ionising Escape Fraction defined by the proportion of photons not absorbed thus escaping to reionise the IGM. By spanning a wide range of these parameters, the LORELI II simulations are representative of a broad range of plausible reionisation scenarios with various reionisation histories and morphologies, leaving distinct imprints on the kSZ signal³.

From the 1106 simulations in which the Gas Conversion Timescale, the Minimum Halo Mass, and the Ionising Escape Fraction are varied, we fit for the overall amplitude α_0 and cut-off scale κ on the electron overdensity power spectra following the procedure described in Gorce et al. (2020). We further select the set of pairs (α_0, κ) corresponding to LORELI II simulations that fall within the $1\text{-}\sigma$ confidence interval of the optical depth τ defined in Sect. 2.1.1, leaving us with 319 simulations. For our fiducial models, we assume $\hat{\alpha} = \langle \log \alpha_0 / \text{Mpc}^3 \rangle = 4.8$ and $\hat{\kappa} = \langle \kappa \rangle = 0.03 \text{ Mpc}^{-1}$, the mean values over our selected 319 simulations.

We compute 11 fiducial kSZ angular power spectra following Gorce et al. (2020) by assuming i) the frequentist best-fit models of Ilić et al. (2025) (corresponding to 11 parameterisations of x_e fitted to *Planck* PR4 data) ii) the mean values $(\hat{\alpha}, \hat{\kappa})$ for all models. The resulting spectra are shown in Fig. 1 (right).

³ We assume in this work that the reionisation histories and the (α_0, κ) are uncorrelated.

Modelling uncertainties The ensemble of 319 pairs allows us to define the range of possible kSZ APS arising from uncertainties in the astrophysical properties of the first sources, namely the dispersion of α_0 and κ in the LORELI II simulations. For a given history of reionisation, we can compute all the 319 kSZ APS assuming the corresponding (α_0, κ) and define an envelope of spectra as our 68% interval.

2.2. Late-time kSZ

For the late-time angular power spectrum component, we assume the analytical shape of Park et al. (2018), in perfect agreement with the simulation of Shaw et al. (2012). We rescale the amplitude following the scaling relation of Shaw et al. (2012) assuming $\tau = 0.058$, $\sigma_8 = 0.8073$, $h = 0.6777$. The best-fit values of τ , σ_8 , and H_0 vary slightly across the $x_e(z)$ models considered (see Fig. 5 in Ilić et al. 2025). However, we find that the resulting variations in the late-time kSZ APS to be negligible ($< 4\%$) compared to variations in the patchy spectra. Our late time kSZ APS is shown in Fig. 1 (dotted line).

3. kSZ signatures of Planck histories of reionisation

3.1. Fiducial kSZ

We show in Fig. 1 the 11 histories of reionisation $x_e(z)$ corresponding to the best fit models of Ilić et al. (2025) (left), as well as the corresponding kSZ angular power spectra, with their patchy (solid and dashed lines) and late (dotted) components, computed with the fiducial $\hat{\alpha}$ and $\hat{\kappa}$ values (right). The kSZ power spectra exhibit two behaviours depending on the duration of the reionisation (as expected, see, e.g., Shaw et al. 2012; Gorce et al. 2020). We highlight the difference between these two sets in Fig. 1 by plotting in dashed lines the ‘short’ reionisation models, and in solid lines the ‘long’ reionisation ones. The total (late + patchy) kSZ APS shown in Fig. 2 exhibit the same behaviour as the patchy kSZ, with ‘long’ history spectra dominated by the patchy part and the ‘short’ by the late contribution.

This result indicates that a kSZ measurement could discriminate between these two broad categories. However, it is obtained for fixed astrophysical parameters. Thus, in the following, we investigate whether the discriminating power of a kSZ measurement is robust to uncertainties on the reionisation history $x_e(z)$ and on the astrophysical parameters (α_0, κ) . To this end, we select one reference model in each group: the hyperbolic tangent \tanh and the 3-point interpolation 3-knots.

3.2. Propagating x_e uncertainties

We propagate the uncertainties in x_e defined in Sec. 2.1.1 by computing the kSZ angular power spectrum for all models within the 68% interval and evaluating the dispersion at each multipole, as shown by the cross-hatched regions in Fig. 2 (middle and right). The ± 0.006 uncertainty in τ (Ilić et al. 2025) from Planck data produces an uncertainty envelope for each kSZ spectrum, but the two groups are still distinguishable.

3.3. Propagating astrophysical uncertainties

Our fiducial assumption for the shape of the electron overdensity power spectrum follows the work of Gorce et al. (2020) and is derived from the mean values of (α_0, κ) in our LORELI II subset (see Sec. 2.1.2). However, this particular (α_0, κ) set may not be representative of our Universe. Thus, we compute, for our two

reference ‘long’ and ‘short’ reionisation histories, the kSZ power spectra of the 319 (α_0, κ) fitted to the LORELI II subset, and show their dispersion in Fig. 2. For both \tanh and 3-knots, we show the resulting uncertainty envelope at each multipole ℓ (vertical hatch in Fig. 2).

We find that, even after marginalising over the range of astrophysical models allowed by the LORELI II simulations, the two groups of reionisation histories remain clearly distinguishable. The resulting envelope widths are comparable to those obtained propagating x_e uncertainties: both sources of uncertainty contribute at a similar level⁴.

Measurements of the kSZ power spectrum could, therefore, provide a powerful discriminant among the reionisation histories allowed by Planck. However, our results are somehow conservative and limited by the fact that we consider independently the two sources of uncertainties, while, in reality, reionisation history and galaxy properties are correlated. More robust estimates, for example marginalising over cosmological parameters or jointly accounting for the correlated uncertainties are required to fully characterise the two-scenario behaviour.

3.4. Could current data discriminate?

We now confront our findings to recent measurements of the kSZ angular power spectrum from the South Pole Telescope (SPT, Chaubal et al. 2026), the Atacama Cosmology Telescope (ACT, Louis et al. 2025), and a joint analysis of Planck, ACT, and SPT data (Tristram et al. 2026; Beringue et al. 2025).

The spectra obtained from fitting the amplitude of a kSZ template to data are compared to our envelopes of allowed spectra in the right panel of Fig. 2. Chaubal et al. (2026) analysed 90, 150, and 220 GHz observations over 1646 deg² from the SPT-3G survey, using several templates of the kSZ signal and other extragalactic foregrounds. With the Agora template (Omori 2024, in red), the data shows better agreement with the ‘long’ reionisation models. In contrast, with the Battaglia et al. (2013) template, both the ACT-DR6 data alone (Louis et al. 2025, in pink) or the combination of Planck, SPT, and ACT data (Tristram et al. 2026, in purple) favour a kSZ amplitude at $\ell = 3000$ which remains below $2.5 \mu\text{K}^2$, even marginalising on other foregrounds (see Beringue et al. 2025; Tristram et al. 2026). The kSZ amplitude is also measured in ℓ -bins in Chaubal et al. (2026), assuming a free shape for the cosmic infrared background (CIB) alone (green crosses) or for both the CIB and the kSZ⁵ (green circles). Both approaches yield spectra that are fully consistent with ‘short’ reionisation scenarios (Fig. 2, middle panel).

Going beyond our reference \tanh and 3-knots x_e models and assuming, for example, the 5 free-CIB points measured by Chaubal et al. (2026), all ‘short’ (‘long’) reionisation histories lead to $\chi^2 < 1.5$ ($\chi^2 > 14$). The same preference remains for sets of measurements shown (except the one coming from the SPT data fit with the Agora template)

Overall, most of the recent measurements favour low kSZ power, which favour ‘short’ reionisation scenarios, although the dispersion between analyses and the associated uncertainties remain significant.

⁴ Note that combining them would require more elaborated propagation as they are weakly degenerated

⁵ Labelled as free CIB ℓ^α G15 SZ and free CIB+SZ in Chaubal et al. (2026), respectively.

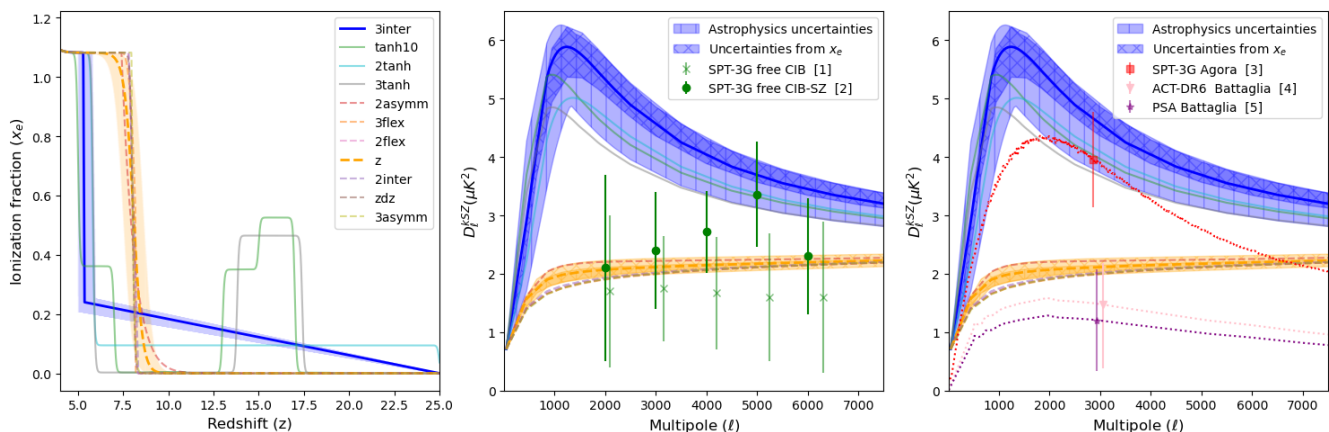


Fig. 2: Same as Fig 1, with our two categories (‘short’ and ‘long’) highlighted in orange and blue, respectively. Left: reionisation histories, with uncertainties from the *Planck* analysis shown as shaded regions. Middle and Right: total (patchy + late) kSZ power spectra, with uncertainties propagated from the x_e uncertainties shown in the left panel (cross-hatched regions), and additional uncertainties arising from the LORELI II–allowed ranges of α_0 and κ (vertical hatched regions). Middle: kSZ spectra compared with binned estimates from SPT-3G. Right: kSZ spectra compared with fitted templates in ACT-DR6, SPT-3G and combined CMB analysis (see text for legends).

4. Discussion and Conclusions

While *Planck* provides robust constraints on the optical depth to reionisation, the detailed shape of the reionisation history remains uncertain. We show that the set of allowed histories can be broadly divided into ‘long’ and ‘short’ scenarios, which produce distinct signatures in the kinetic Sunyaev–Zel’dovich power spectrum.

Assuming a fixed cosmology corresponding to the concordance Λ CDM model, we investigate how uncertainties propagate from two sources: the determination of the best-fit reionisation history, $x_e(z)$, from large-scale CMB data, and the allowed range of galaxy properties within the LORELI II simulation suite. Restricting our analysis to 68% confidence intervals, we find that these two sources of uncertainty contribute comparably to the dispersion of the kSZ angular power spectrum. However, even after propagating these uncertainties, the two classes of reionisation histories remain clearly distinguishable. We found that a discrimination at a 5σ level could be obtained, if an experiment could measure the total kSZ angular power spectrum at $\ell \sim 2000$ with a sensitivity of $\sim 0.4 \mu\text{K}^2$.

Unfortunately, current measurements of the kSZ angular power spectrum span a wide range ($\sim 0 - 3 \mu\text{K}^2$), and are therefore not yet sufficient to discriminate between reionisation histories. Although most analyses appear to favour ‘short’ reionisation scenarios, a comprehensive analysis simultaneously probing cosmology, reionisation history, kSZ amplitude, and associated systematics is required to draw firm conclusions. Following previous studies (Douspis et al. 2022; Gorce et al. 2022), recently developed joint likelihood combining *Planck* and ACT, together with the latest SPT-3G measurements (e.g. Tristram et al. 2026), could be exploited to perform such an analysis and extract a maximum of information from current data, before Stage 4 and 5 telescopes going online.

Indeed, eventually, kSZ measurements could further discriminate between reionisation histories within a subgroup and provide the shape of the reionisation history as a function of redshift. However, we find that variations between models within the same group are at the level of $\sim 10\%$, implying that observational data must reach at least this level of sensitivity to effectively discriminate between them.

Other observations, such as the quasar damping wing, the Lyman- α forest, or high-redshift galaxy luminosity functions, may also soon help discriminate between these scenarios, until a measurement of the high-redshift 21 cm signal provides the full shape of the reionisation history.

Acknowledgements. The authors acknowledge the support of the French Agence Nationale de la Recherche (ANR), under grant ANR-22-CE31-0010 (project BATMAN). This work was supported by the ‘‘action th ematique’’ Cosmology-Galaxies (ATCG) of the CNRS/INSU PN Astro and ANR PIA funding ANR-20-IDEE-0002. We also acknowledge the use of many open-source libraries, including CAMB (Lewis et al. 2000), numpy (Harris et al. 2020) and matplotlib (Hunter 2007).

References

- Battaglia, N., Natarajan, A., Trac, H., Cen, R., & Loeb, A. 2013, *ApJ*, 776, 83
 Beringue, B., Surrao, K. M., Hill, J. C., et al. 2025, *J. Cosmology Astropart. Phys.*, 2025, 082
 Chaubal, P., Huang, N., Reichardt, C. L., et al. 2026, arXiv e-prints, arXiv:2601.20551
 Douspis, M., Salvati, L., Gorce, A., & Aghanim, N. 2022, *Astronomy & Astrophysics*, 659, A99
 Genesini, V., Galloni, G., Pagano, L., Campeti, P., & Lattanzi, M. 2026, arXiv e-prints, arXiv:2603.22454
 Gorce, A., Douspis, M., & Salvati, L. 2022, *A&A*, 662, A122
 Gorce, A., Ilić, S., Douspis, M., Aubert, D., & Langer, M. 2020, *A&A*, 640, A90
 Harris, C. R., Millman, K. J., van der Walt, S. J., et al. 2020, *Nature*, 585, 357
 Hunter, J. D. 2007, *Computing in Science & Engineering*, 9, 90
 Ilić, S., Tristram, M., Douspis, M., et al. 2025, *A&A*, 700, A26
 Lewis, A., Challinor, A., & Lasenby, A. 2000, *ApJ*, 538, 473
 Louis, T., La Posta, A., Atkins, Z., et al. 2025, *J. Cosmology Astropart. Phys.*, 2025, 062
 McBride, L., Gorce, A., Douspis, M., et al. 2025, arXiv e-prints, arXiv:2511.22309
 Meriot, R. & Semelin, B. 2024, *A&A*, 683, A24
 Meriot, R., Semelin, B., & Cornu, D. 2025, *A&A*, 698, A80
 Omori, Y. 2024, *MNRAS*, 530, 5030
 Pagano, L., Delouis, J. M., Mottet, S., Puget, J. L., & Vibert, L. 2020, *A&A*, 635, A99
 Paradiso, S., Colombo, L. P. L., Andersen, K. J., et al. 2023, *A&A*, 675, A12
 Park, H., Alvarez, M. A., & Bond, J. R. 2018, *ApJ*, 853, 121
 Planck Collaboration VI. 2020, *A&A*, 641, A6
 Planck Collaboration Int. XLVII. 2016, *A&A*, 596, A108
 Planck Collaboration Int. LVII. 2020, *A&A*, 643, A42
 Reichardt, C., Patil, S., Ade, P., et al. 2021, *The Astrophysical Journal*, 908, 199
 Shaw, L. D., Rudd, D. H., & Nagai, D. 2012, *ApJ*, 756, 15
 Sunyaev, R. & Zeldovich, Y. B. 1980, *Monthly Notices of the Royal Astronomical Society*, vol. 190, Feb. 1980, p. 413-420., 190, 413
 Tristram, M., Douspis, M., Gorce, A., et al. 2026, *A&A* in press, 0
 Zahn, O., Reichardt, C. L., Shaw, L., et al. 2012, *ApJ*, 756, 65
 Zeldovich, Y. B. & Sunyaev, R. A. 1969, *Ap&SS*, 4, 301